3
Temporal quantum correlations in subatomic systems

In this chapter, we investigate various temporal quantum correlations quantified by different avatars of Leggett-Garg inequality in subatomic systems like neutrinos and neutral mesons. The chapter is based on articles [27, 28, 54–56]

3.1 Dynamics of the relevant subatomic systems

This chapter is devoted to a study of temporal quantum correlations using various avatars of Leggett-Garg inequality in subatomic systems. To this end we first give a brief description of the dynamics of the relevant systems.

Neutrino dynamics: The non zero mass square differences lead to the phenomena of neutrino oscillation, the existence of a flavor state $|\nu_\alpha\rangle$ into a coherent superposition of mass eigen states $|\nu_k\rangle$

$$|\nu_\alpha\rangle = \sum_k U^*_{\alpha k} |\nu_k\rangle \,. \tag{3.1}$$

where $U_{\alpha k}$ are the elements of a 3×3 unitary PMNS (Pontecorvo-Maki-Nakagawa-Sakata) mixing matrix U parameterized by three mixing angles ($\theta_{12},\ \theta_{23},\ \theta_{13}$) and a CP violating phase δ. A convenient parametrization for $U(\theta_{12}, \theta_{23}, \theta_{32}, \delta)$ is given by

$$U(\theta_{12}, \theta_{23}, \theta_{32}, \delta) = \begin{pmatrix} c_{12}c_{13} & s_{12}c_{13} & s_{23}e^{-i\delta} \\ -s_{12}c_{23} - c_{12}s_{23}s_{13}e^{i\delta} & c_{12}c_{23} - s_{12}s_{23}s_{13}e^{i\delta} & s_{23}c_{13} \\ s_{12}s_{23} - c_{12}c_{23}s_{13}e^{i\delta} & -c_{12}s_{23} - s_{12}c_{23}s_{13}e^{i\delta} & c_{23}c_{13} \end{pmatrix}, \tag{3.2}$$

where $c_{ij} = \cos\theta_{ij}$, $s_{ij} = \sin\theta_{ij}$, θ_{ij} being the mixing angles and δ the CP violating phase. The experimental values for the PMNS mixing matrix are taken from the particle data group [255]. Eq. (3.1) represents the state of the neutrino at time $t = 0$. At a later time t, the flavor state evolves into

$$|\nu_\alpha(t)\rangle = \sum_k U^*_{\alpha k} e^{-iE_k t} |\nu_k\rangle = \sum_\beta \mathcal{A}_{\nu_\alpha \to \nu_\beta}(t) |\nu_\beta\rangle \,, \tag{3.3}$$

where we have expanded $|\nu_\alpha\rangle$ in terms of the energy (mass) eigenstates $|\nu_k\rangle$, which evolve independently under Schrödinger equation. This leads to the amplitudes $\mathcal{A}_{\nu_\alpha \to \nu_\beta}$, of transition from flavor ν_α to ν_β, given by

$$\mathcal{A}_{\nu_\alpha \to \nu_\beta}(t) = \sum_k U_{\beta k} e^{-iE_k t} U^*_{\alpha k}. \tag{3.4}$$

Consequently, the probability of transition is given by

$$P_{\nu_\alpha \to \nu_\beta}(t) = |\mathcal{A}_{\nu_\alpha \to \nu_\beta}(t)|^2 = |\sum_k U_{\beta k} e^{-iE_k t} U^*_{\alpha k}|^2. \tag{3.5}$$

Here, use has been made of the ultra-relativistic approximation $t \approx L$, where L is the distance traveled by the neutrino. The amplitudes $\mathcal{A}_{\nu_\alpha \to \nu_\beta}(t)$ form the elements of the so called flavor evolution matrix $U_f(t)$. In matrix notation the state represented by the vector $\boldsymbol{\nu}_\alpha(t) \equiv (\nu_e(t) \;\; \nu_\mu(t) \;\; \nu_\tau(t))^T$, where T is the transposition operation, is connected to the state at $t = 0$ by

$$\boldsymbol{\nu}_\alpha(t) = U_f(t)\boldsymbol{\nu}_\alpha(0). \tag{3.6}$$

Neutrinos propagating through a constant matter density (with electron density N_e) interact weakly with electrons. This interaction is characterized by the matter density parameter $A = \pm\sqrt{2}G_F N_e$, interact weakly with the electrons in the medium. As a result of this interaction, the Hamiltonian $H_m = \mathrm{diag}[E_1, E_2, E_3]$ (in mass basis) picks up an interaction term $V_f = \mathrm{diag}[A, 0, 0]$ (in flavor basis). This leads to the following form of the flavor evolution matrix [256]

$$U_f(L) = \phi \sum_{n=1}^{3} \frac{e^{-i\lambda_n L}}{3\lambda_n^2 + c_1} \left[(\lambda_n^2 + c_1)\mathbf{I} + \lambda_n \tilde{T} + \tilde{T}^2\right], \tag{3.7}$$

The phase $\phi = e^{-i\frac{Tr\mathcal{H}_m}{3}L}$, $c_1 = det(T)tr(T^{-1})$ and the Hamiltonian in mass basis is $\mathcal{H}_m = H_m + U^{-1}V_f U$. The λ_n are the eigenvalues of T and the matrix T and $\tilde{T}$ are given in [256]. The flavor evolution operator, defined in Eq. (3.7), can be used to deal with the situation when neutrinos pass through a series of matter densities with the matter density parameters $A_1, A_2, \ldots, A_n$. In this case, the total evolution operator becomes

$$U_f^{\mathrm{tot}}(L) = \prod_{i=1}^{n} U_f(L_i). \tag{3.8}$$

Here, $L = \sum_{i=1}^{n} L_i$ and $U_f(L_i)$ is evaluated for the density parameter A_i. A useful application of Eq. (3.8) has been suggested for the mantle-core-mantle step function model simulating the Earth's matter density profile [257].

Meson dynamics: We describe briefly the time evolution of $B^o(K^o)$ neutral meson system. Since both B^o and K^o share the same scheme of dynamics, we discuss only B^o system and the results, with appropriate notational changes, will be applicable to the K^o system. The states of the total system, including the meson and the vacuum $|0\rangle$, introduced in order to incorporate the effect of decay in the meson system, reside in the Hilbert space given by the direct sum $\mathcal{H}_{B^0} \oplus \mathcal{H}_0$ of Hilbert spaces of meson state $\mathcal{H}_{B^0}$ and zero particle vacuum state $\mathcal{H}_0$ [10, 258, 259]. The total space is spanned by the orthonormal vectors $|B^0\rangle$, $|\bar{B}^0\rangle$ and $|0\rangle$

$$|B^0\rangle = \begin{pmatrix}1\\0\\0\end{pmatrix}; \quad |\bar{B}^0\rangle = \begin{pmatrix}0\\1\\0\end{pmatrix}; \quad |0\rangle = \begin{pmatrix}0\\0\\1\end{pmatrix}. \tag{3.9}$$

Here B^0 stands for B_d^0/B_s^0 mesons. The mass eigenstates $\{|B_L\rangle, |B_H\rangle\}$ are related to the flavor eigenstates $\{|B^o\rangle, |\bar{B}^o\rangle\}$ by the equations

$$|B_L\rangle = p\,|B^o\rangle + q\,|\bar{B}^o\rangle, \qquad |B_H\rangle = p\,|B^o\rangle - q\,|\bar{B}^o\rangle, \tag{3.10}$$

with $|p|^2+|q|^2=1$. The time evolution is given by a family of completely positive trace preserving maps forming a one parameter dynamical semigroup. The complete positivity requires the time evolution of a state of the system being represented by the operator-sum representation [216]

$$\rho(t)=\sum_{i=0} E_i(t)\rho(0)E_i^{\dagger}(t), \tag{3.11}$$

where the $Kraus$ operators have the following form

$$\begin{aligned}
E_0 &= |0\rangle\langle 0|\,,\\
E_1 &= \mathcal{E}_{1+}\big(|B^0\rangle\langle B^0|+|\bar{B}^0\rangle\langle\bar{B}^0|\big)+\mathcal{E}_{1-}\big(\frac{p}{q}|B^0\rangle\langle\bar{B}^0|+\frac{q}{p}|\bar{B}^0\rangle\langle B^0|\big),\\
E_2 &= \mathcal{E}_2\big(\frac{p+q}{2p}|0\rangle\langle B^0|+\frac{p+q}{2q}|0\rangle\langle\bar{B}^0|\big),\\
E_3 &= \mathcal{E}_{3+}\frac{p+q}{2p}|0\rangle\langle B^0|+\mathcal{E}_{3-}\frac{p+q}{2q}|0\rangle\langle\bar{B}^0|\,,\\
E_4 &= \mathcal{E}_4\big(|B^0\rangle\langle B^0|+|\bar{B}^0\rangle\langle\bar{B}^0|+\frac{p}{q}|B^0\rangle\langle\bar{B}^o|+\frac{q}{p}|\bar{B}^0\rangle\langle B^0|\big),\\
E_5 &= \mathcal{E}_5\big(|B^0\rangle\langle B^0|+|\bar{B}^0\rangle\langle\bar{B}^0|-\frac{p}{q}|B^0\rangle\langle\bar{B}^0|-\frac{q}{p}|\bar{B}^0\rangle\langle B^0|\big).
\end{aligned}$$

Here the coefficients are

$$\mathcal{E}_{1\pm}=\frac{1}{2}\left[e^{-(2im_L+\Gamma_L+\lambda)t/2}\pm e^{-(2im_H+\Gamma_H+\lambda)t/2}\right], \tag{3.12a}$$

$$\mathcal{E}_2=\sqrt{\frac{Re[\frac{p-q}{p+q}]}{|p|^2-|q|^2}\big(1-e^{-\Gamma_L t}-(|p|^2-|q|^2)^2\frac{|1-e^{-(\Gamma+\lambda-i\Delta m)t}|^2}{1-e^{-\Gamma_H t}}\big)}, \tag{3.12b}$$

$$\mathcal{E}_{3\pm}=\sqrt{\frac{Re[\frac{p-q}{p+q}]}{(|p|^2-|q|^2)(1-e^{-\Gamma_H t})}}\big[1-e^{-\Gamma_H t}\pm(1-e^{-(\Gamma+\lambda-i\Delta m)t})(|p|^2-|q|^2)\big], \tag{3.12c}$$

$$\mathcal{E}_4=\frac{e^{-\Gamma_L t/2}}{2}\sqrt{1-e^{-\lambda t}}, \tag{3.12d}$$

$$\mathcal{E}_5=\frac{e^{-\Gamma_H t/2}}{2}\sqrt{1-e^{-\lambda t}}. \tag{3.12e}$$

A meson initially in state $\rho_{B^0}(0)=|B^0\rangle\langle B^0|$ or $\rho_{\bar{B}^0}(0)=|\bar{B}^0\rangle\langle\bar{B}^0|$, after time t, evolves to

$$\rho_{B^0}(t)=\frac{1}{2}e^{-\Gamma t}\begin{pmatrix} a_{ch}+e^{-\lambda t}a_c & (\frac{q}{p})^*(-a_{sh}-ie^{-\lambda t}a_s) & 0\\ (\frac{q}{p})(-a_{sh}+ie^{-\lambda t}a_s) & |\frac{q}{p}|^2a_{ch}-e^{-\lambda t}a_c & 0\\ 0 & 0 & \rho_{33}(t)\end{pmatrix}, \tag{3.13}$$

and

$$\rho_{\bar{B}^0}(t)=\frac{1}{2}e^{-\Gamma t}\begin{pmatrix} |\frac{p}{q}|^2(a_{ch}-e^{-\lambda t}a_c) & (\frac{p}{q})(-a_{sh}+ie^{-\lambda t}a_s) & 0\\ (\frac{p}{q})^*(-a_{sh}-ie^{-\lambda t}a_s) & a_{ch}+e^{-\lambda t}a_c & 0\\ 0 & 0 & \tilde{\rho}_{33}(t)\end{pmatrix}. \tag{3.14}$$

Here, a_{ch} (a_{sh}) and a_c (a_s) stand for the hyperbolic functions $\cosh[\frac{\Delta\Gamma t}{2}]$ ($\sinh[\frac{\Delta\Gamma t}{2}]$) and the trigonometric functions $\cos[\Delta m t]$ ($\sin[\Delta m t]$), respectively. p and q are defined in Eq. (3.10). $\Delta\Gamma=\Gamma_L-\Gamma_H$ is the difference of the decay width Γ_L (for B_L^o) and Γ_H (for B_H^o). $\Gamma=\frac{1}{2}(\Gamma_L+\Gamma_H)$ is the average decay width. The mass difference $\Delta m=m_H-m_L$, where

m_H and m_L are the masses of B_H^o and B_L^o states, respectively. The strength of the interaction between the one particle system and its environment is quantified by λ, the *decoherence* parameter [260]. The elements $\rho_{33}(t)$ and $\tilde{\rho}_{33}(t)$ are known functions of B physics parameters, not used in this work. In the following section, we use this formalism to develop the LGI and LGtI for the meson systems.

3.2 Detailed study of various temporal quantum correlations

Having spelled out the dynamics of neutrino and meson systems, we present a detailed investigation of various temporal quantum correlations described in Sec. 2.6.1.

1. **Temporal quantum correlations in neutrino system:**

   Here, we discuss various temporal quantum correlation in three flavor neutrino system in the context of some well know neutrino experiments like DUNE (Deep Underground Neutrino Experiment), NOνA (NuMI Off-axis ν_e Appearance), and T2K (Tokai to Kamioka). DUNE facility is located at Stanford Underground Research Laboratory at South Dakota and will have access to a rather wide band energy $1 - 10$ GeV. The current accelerator neutrino experiments, T2K and NOνA, both have rather narrow energy bands. For T2K, the baseline is 295 km and the energy range is $0.5 - 2$ GeV. For NOνA, the corresponding numbers are 810 km and $1 - 4$ GeV. These (T2K and NOνA) experiments were planned before the mixing angle θ_{13} was measured to be moderately large. Their neutrino beams were designed to be narrow band beams to suppress the backgrounds.

   Standard Leggett-Garg Inequality: In this subsection we characterize the LG parameter K_3, defined in Eq. (2.23), in the case of three-flavor neutrinos and study the validity of LGI using input parameters from two of the current major experimental platforms, namely NOνA and T2K and the future experiment DUNE. Therefore, we focus on having a specific initial flavor eigenstate, i.e. ν_μ, and choose equal time intervals ($t_0 = 0, t_1 = t, t_2 = 2t$). Herewith, our LG parameter K_3 becomes the sum of the following correlation functions

   $$K_3 = C(0,t) + C(t,2t) - C(0,2t) \leq 1 \ . \tag{3.15}$$

   To compute the two-time correlation functions C we need to employ the dichotomic observable $\hat{Q} = 2\,|\nu_\alpha\rangle\,\langle\nu_\alpha| - \mathbf{1}$, which physically corresponds to asking whether the neutrino is still in the state $|\nu_\mu\rangle$ (associated outcome 1) or has undergone a transition to another flavor state $|\nu_\alpha\rangle$ with $\alpha \neq \mu$ (associated outcome -1). Straightforwardly one finds for

   $$\begin{aligned} C(0,t) &= 4\delta_{\alpha\mu}\langle\nu_\mu(t)|\nu_\alpha\rangle\langle\nu_\alpha|\nu_\mu(t)\rangle - 2\langle\nu_\mu(t)|\nu_\alpha\rangle\langle\nu_\alpha|\nu_\mu(t)\rangle - 2\delta_{\alpha\mu} + 1 \\ &= \begin{cases} 2\mathcal{P}_{\mu\to\mu}(t) - 1 & \text{for } \alpha = \mu \\ \\ 1 - 2\mathcal{P}_{\mu\to\alpha}(t) & \text{for } \alpha \neq \mu, \end{cases} \end{aligned} \tag{3.16}$$

   where $\mathcal{P}_{\mu\to\mu}(t)$ is the surviving probability and $\mathcal{P}_{\mu\to\alpha}(t)$ is the transition probability. Use has been made of the fact that the completeness condition in three flavor neutrino oscillation is $\sum_{\alpha=e,\mu,\tau} |\nu_\alpha\rangle\,\langle\nu_\alpha| = \mathbf{1}$, leading to $P_{\mu e}(t) + P_{\mu\mu}(t) + P_{\mu\tau}(t) = 1$ in Eq. (3.16).

   The probabilities with matter effect, depend on the neutrino energy E, the mass square differences $\Delta_{ij} = m_j^2 - m_i^2$, the matter density parameter A, the mixing angles θ_{ij} and the CP violating phase δ, i.e., $\mathcal{P}_{\mu\to\alpha} = \mathcal{P}_{\mu\to\alpha}(E, t, A, \Delta_{12}, \Delta_{31}, \theta_{12}, \theta_{23}, \theta_{13}, \delta)$. For brevity in nomenclature, we suppress all the other dependencies except the time dependence. The ongoing neutrino experiments NOνA and T2K studying the transition probabilities, $P_{\mu\to e}(t)$. Thus we focus on the choice $\alpha = e$ in the following.

The tricky part is the correlation $C(t, 2t)$ since it cannot be re-written into surviving or/and transition probabilities if one does not invoke the stationary condition, i.e. considering Legett-Garg type inequalities which has been done in details in [27], and is discussed ahead. The correlation function computes to

$$C(t, 2t) = 1 - 2P_{\mu\to e}(t) - 2P_{\mu\to e}(2t) + 4\alpha(t)P_{\mu\to e}(2t) + 4\beta(t). \tag{3.17}$$

Finally, our LG function is given by

$$K_3 = 1 - 4P_{\mu\to e}(t) + 4\alpha(t)P_{\mu\to e}(2t) + 4\beta(t), \tag{3.18}$$

with

$$\alpha(t) = |U_f^{11}(t)|^2, \tag{3.19}$$

$$\beta(t) = Re\Big[U_f^{11}(t)\bar{U}_f^{21}(t)U_f^{22}(2t)\bar{U}_f^{12}(2t) + U_f^{11}(t)\bar{U}_f^{31}(t)U_f^{32}(2t)\bar{U}_f^{12}(2t)\Big]. \tag{3.20}$$

Here $\bar{U}_f^{ij} = U_f^{ij*}$ represents the complex conjugate of U_f^{ij}, the ij-th element of the flavor evolution matrix U_f defined in Eq. (3.6). The parameters α and β, apart from time t, also depend on the energy of neutrino and the mixing angles and mass square differences. Also α, unlike β, is independent of the CP violating phase δ. The term β is not in the form of probabilities and therefore cannot be measured with the present day neutrino experimental facilities.

It should be noticed that for $\alpha = 0.5$ and $\beta = 0$, we recover the *stationarity* limit of LGI given by Eq. (2.25). An important observation is that for higher energies, the interference term β converges to zero. Also, the term α, which varies between zero and one, averages to $\frac{1}{2}$, thereby taking LGI to LGtI. Therefore, LGtI can be thought of as a kind of LGI for higher neutrino energies.

Stationarity assisted LGI: Under the *stationary* assumption, the autocorrelation functions $C(t_i, t_j) \equiv C(0, t)$ are straightforwardly found and can be compactly expressed in terms of the probability $P_{\alpha\to\beta}(t) = |\langle\nu_\beta(t)|\nu_\alpha(0)\rangle|^2$ as

$$C(0, t) = 1 - 2P_{\alpha\to\beta}(t). \tag{3.21}$$

Note that both the survival probability $P_{\alpha\to\alpha}(t)$ and the transition probability $P_{\alpha\to\beta}(t)$ actually depend on many physical parameters such as the neutrino energy E, the mass square differences $\Delta_{ij} = m_j^2 - m_i^2$, the matter potential A, the mixing angles θ_{ij} and the CP violating phase δ. For clarity of notation, however, we will keep the dependence on all these parameters implicit except for the energy E, for reasons that will be clear in a short-while. Care, however, should be taken when moving from neutrinos to anti-neutrinos since both the CP violating phase δ and the matter potential A reverse their signs [261]. The quantity of interest thus becomes

$$K_3 = 1 + 2P_{\alpha\to\beta}(2t, E) - 4P_{\alpha\to\beta}(t, E), \tag{3.22}$$

which shows its experimental feasibility, being clearly expressed only in terms of measurable quantities, i.e., survival and transition probabilities.

In light of its physical grasp, the following considerations on Eq. (3.22) naturally follow. Neutrino oscillation experiments typically operate in the ultra-relativistic regime and therefore the time-dependence in the probabilities $P_{\alpha\to\beta}(t, E)$ can be equivalently replaced by

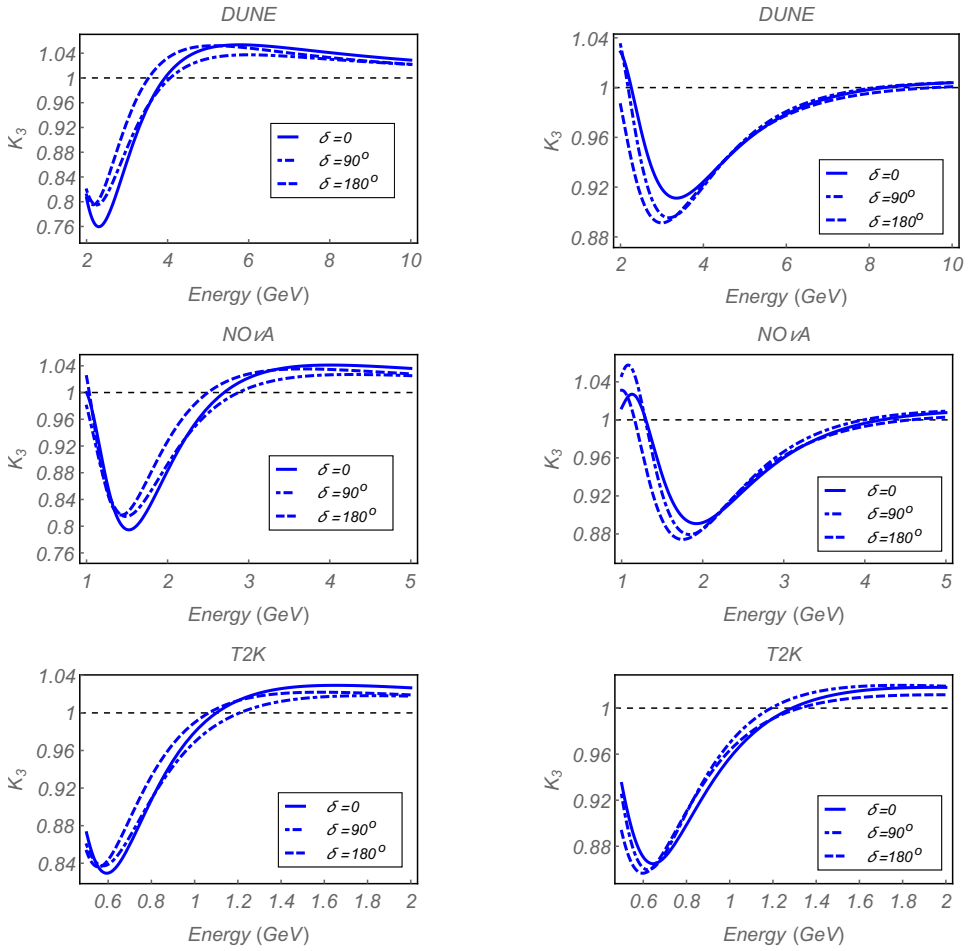

Figure 3.1: Leggett-Garg function K_3 plotted against energy for DUNE (top), NOνA (middle) and T2K (bottom) experimental set-ups for different values of the CP violating phase δ. The left and right panels correspond to the initial neutrino and antineutrino state, respectively. The sign of Δ_{31} is taken to be positive. The time can be identified with the length (baseline) which is 1300 km, 810 km and 295 km for DUNE, NOνA and T2K, respectively.

the length L travelled by neutrinos [262]. An experimental verification of Eq. (3.22) would thus require two detectors placed at L and $2L$, respectively. The current experimental facilities, however, do not allow for such a setup. It is nevertheless possible to bypass such an obstacle by looking for matching energies $\tilde{E}$ satisfying the implicit equation

$$P_{\alpha\to\beta}(2L, E) \;\equiv\; P_{\alpha\to\beta}(L, \tilde{E}). \tag{3.23}$$

Let us remark here that of course this identification can lead to multiple solutions and both probabilities may not have the support on the same interval of energies. Further, it is worth mentioning that in case of vacuum oscillations, energies E and $\tilde{E}$ are related as $\tilde{E} = E/2$. However, in presence of the matter effect, this relation does not hold and $\tilde{E}$ has to be calculated by Eq. (3.23). Given that the matter modified oscillation probability is a smooth function of energy, it is always possible to find an $\tilde{E}$ which satisfies Eq. (3.23).

Now we are ready to exploit our result Eq. (3.22) for neutrinos and antineutrinos and to connect it to the experiments via Eq. (3.23). The experiments under consideration employ $\nu_\mu/\bar{\nu}_\mu$ beams as sources and study the survival probabilities $P(\nu_\mu \to \nu_\mu)(t, E)$ and $P(\bar{\nu}_\mu \to \bar{\nu}_\mu)(t, E)$ and also the transition probabilities $P(\nu_\mu \to \nu_e)(t, E)$ and $P(\bar{\nu}_\mu \to \bar{\nu}_e)(t, E)$. In

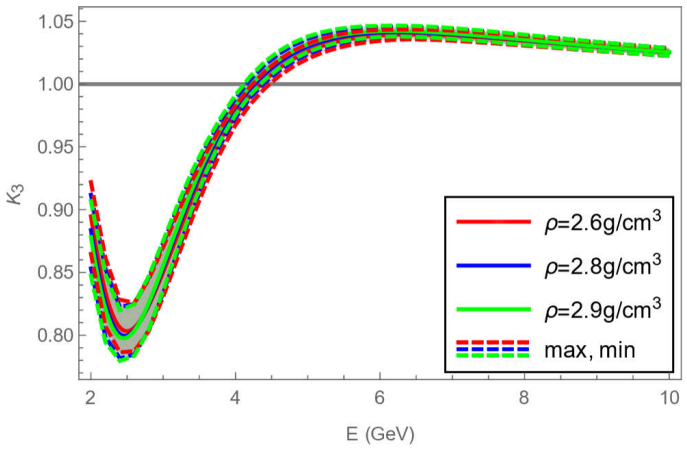

Figure 3.2: The LG parameter K_3 plotted for different values of the matter density $\rho = 2.6/2.8/2.9 g/cm^3$ with the matter potential $A = A(\rho)$ in dependence of the energy E and including the known errors for the other parameters, i.e. the three mixing angles θ_{ij} and the three mass differences Δ_{ij} given in Ref. [255]. Mean values of the three mixing angles θ_{ij} and the three mass differences Δ_{ij} are taken according to Ref. [255] as well. The (dotted) curves correspond to the mean values for which the lower and upper possible value for the errors were computed numerically. A length L of 1300 km and a CP violating phase δ of 0 are considered.

this work, we concentrate on the transition probabilities, which are sensitive to matter effects and CP violation in long baseline accelerator neutrino experiments. We evaluate

$$K_3 = 1 + 2P_{\mu\to e}(L, \tilde{E}) - 4P_{\mu\to e}(L, E), \tag{3.24}$$

for both neutrinos and anti-neutrinos. In each case, the calculation is done for both positive and negative values of $\pm\Delta_{31}$ and for a given matter potential A.

Let us first investigate the sensitivity of K_3 to the matter potential A as a function of the energy E by taking into account the errors in the mixing and mass squared differences, which is displayed in Fig. 3.2. For high energies the quantity K_3 depends less on the uncertainties in the experimental values and a clear violation is observed. The dependence of the function K_3 on the experimental uncertainties is higher for lower energies and no violation is found below a certain energy.

In Fig. (3.3), we plot the maximum of K_3 over a certain energy interval ΔE which is identified with a certain energy interval $\Delta\tilde{E}$, Eq. (3.23), as function of the CP violating parameter δ. More explicitly, the maximization is performed for a given A, Δ_{31} at fixed values of the CP violating phase $\{\delta_k\}$ and within the energy window of the experimental setup. It is also worth stressing that the value of $\tilde{E}$ is found by solving Eq. (3.23) after imposing the above constraints on the mass square difference Δ_{31} and $\delta = \delta_k$.

Two interesting features stand out from Fig. 3.3. Maximum value of K_3 for neutrinos is larger (smaller) for δ in the lower (upper) half plane. This is a reflection of the dependence of $P(\nu_\mu \to \nu_e)$ on δ. More interestingly, the K_3 violation in neutrinos is nearly an order of magnitude larger for the case of positive Δ_{31} compared to the case of negative Δ_{31}. The situation is reversed for anti-neutrinos. These plots indicate that one should attempt to measure K_3 using neutrino data for which Δ_{31} is positive, whereas the anti-neutrino data should be used for such an attempt when Δ_{31} turns out to be negative. Fig. 3.4 depicts the maximum of K_3 for T2K and NOνA experiments for the parameters (energy, baseline and

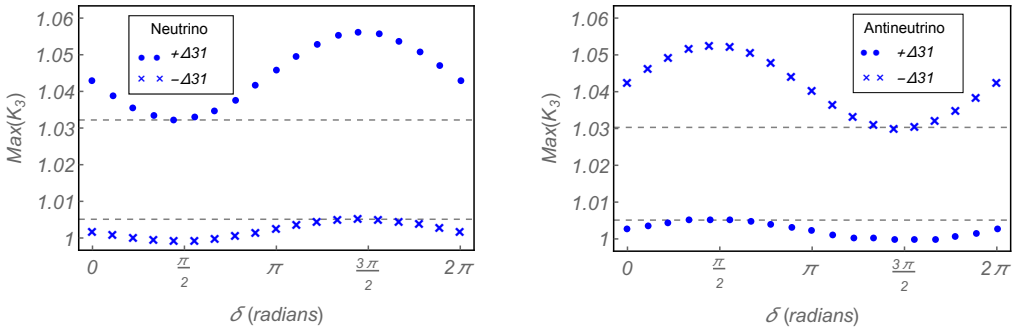

Figure 3.3: DUNE: Maximum of K_3 plotted against CP violating phase δ in the presence of matter effects ($\rho = 2.8 g/cm^3$). Dotted and crossed curves correspond to the positive and negative signs of Δ_{31}, respectively. Length L is equal to 1300 km and the neutrino energy E is varied between 2 GeV to 10 GeV. The corresponding range of $\tilde{E}$ is 1 to 5 GeV. The left and right panels correspond to neutrinos (positive mass density $+A$ and positive CP violating phase δ) and anti-neutrinos ($-A$, $-\delta$), respectively. The horizontal dashed lines highlight the lower and upper bounds of LGI with normal and inverted mass hierarchy in DUNE.

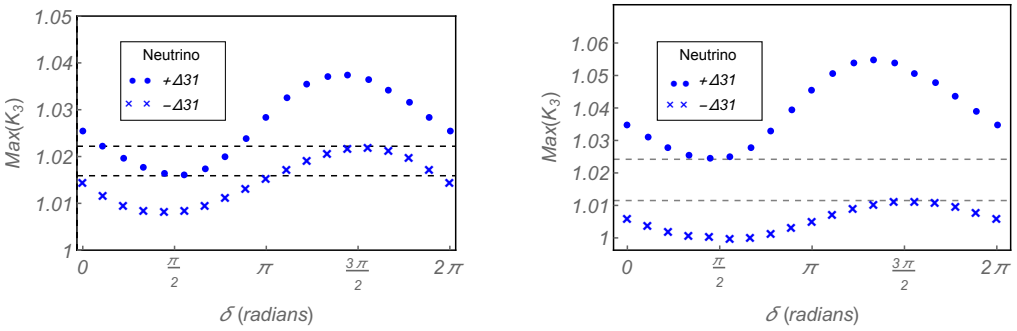

Figure 3.4: T2K and NOνA: Maximum of the parameter K_3 plotted vs CP violating phase δ for T2K (left panel) and NOνA (right panel). Dotted and crossed curves correspond to the positive and negative signs of Δ_{31}, respectively. Length L is 295 km and 810 km for T2K and for NOvA, respectively. The energy E is varied between 1 GeV to 2 GeV for T2K with $\tilde{E}$ between 0.1 GeV to 1 GeV, while for NOνA E is taken between 1.5 GeV to 5 GeV with $\tilde{E}$ between 0.1 GeV to 3 GeV. In case of T2K, the region between the dashed horizontal lines, is not able to distinguish the normal and inverted mass hierarchy.

matter density) of the latest neutrino runs. The corresponding plots for anti-neutrino run can be obtained from Fig. 3.4 by changing sign of the matter density parameter A and replacing δ by $2\pi - \delta$, as in the case of DUNE.

We see that the plots for positive and negative values of Δ_{31} are well separated in the case of NOνA whereas the separation is much less for the case of T2K. This is a consequence of the matter effect for T2K being much less than that of NOνA. It is clear from the above discussions, that owing to the wide energy band, DUNE experiment is suitable for studying K_3 and its sensitivity to the neutrino mass-hierarchy and CP symmetry violations. Further, the violation of the LGtI is significant in $\nu_\mu \to \nu_e$ ($\bar{\nu}_\mu \to \bar{\nu}_e$) transitions for normal (inverted) mass-hierarchy.

Entropic form of LGI: Let us assume that we have prepared an ensemble of neutrinos all existing in a *fixed* flavor state, say ν_α ($\alpha = e, \mu, \tau$), at time t_i. We choose the projector

$\Pi = |\nu_\beta\rangle\langle\nu_\beta|$, which projects a particular flavor state $|\nu_\beta\rangle$ ($\beta = e, \mu, \tau$). In Heisenberg picture, $\Pi(t) = U_f^\dagger(t)\Pi U_f(t)$. For brevity, let us use the notation α_j to denote the flavor state $|\nu_\alpha\rangle$ at time t_j. The conditional probability of obtaining outcome α_{j+1} at time t_{j+1} given that α_j was obtained at time t_j is given by

$$\begin{aligned} P(\alpha_{j+1}, t_{j+1}|\alpha_j, t_j) &= Tr[\rho'\Pi_{\alpha_{j+1}}(t_{j+1})] = Tr[\frac{\Pi_{\alpha_j}(t_j)\rho(0)\Pi_{\alpha_j}(t_j)}{Tr[\rho(0)\Pi_{\alpha_j}(t_j)]}\Pi_{\alpha_{j+1}}(t_{j+1})], \\ &= Tr[\frac{\Pi_{\alpha_j}(t_j)\rho(0)\Pi_{\alpha_j}(t_j)}{P_{\alpha_j}(t_j)}\Pi_{\alpha_{j+1}}(t_{j+1})]. \end{aligned} \tag{3.25}$$

Here ρ' is the state after the projective measurement made at time t_j and is given by $\frac{\Pi_{\alpha_j}(t_j)\rho(0)\Pi_{\alpha_j}(t_j)}{Tr[\rho\Pi_{\alpha_j}(t_j)]}$. The joint probability, therefore becomes

$$\begin{aligned} &P(\alpha_j, \alpha_{j+1}) \\ &= Tr[\Pi_{\alpha_j}(t_j)\rho(0)\Pi_{\alpha_j}(t_j)\Pi_{\alpha_{j+1}}(t_{j+1})], \\ &= Tr[U_f^\dagger(t_j)\,|\alpha_j\rangle\,\langle\alpha_j|\,U_f(t_j)\rho(0)U_f^\dagger(t_j)\,|\alpha_j\rangle\,\langle\alpha_j|\,U_f(t_j)U_f^\dagger(t_{j+1})\,|\alpha_{j+1}\rangle\,\langle\alpha_{j+1}|\,U_f(t_{j+1})], \\ &= Tr[|\alpha_j\rangle\,\langle\alpha_j|\,U_f(t_j)\rho(0)U_f^\dagger(t_j)\,|\alpha_j\rangle\,\langle\alpha_j|\,U_f(t_j)U_f^\dagger(t_{j+1})\,|\alpha_{j+1}\rangle\,\langle\alpha_{j+1}|\,U_f(t_{j+1})U_f^\dagger(t_j)], \\ &= \langle\alpha_j|\rho(t_j)|\alpha_j\rangle\,|\langle\alpha_{j+1}|U_f(t_{j+1})U_f^\dagger(t_j)|\alpha_j\rangle|^2. \end{aligned} \tag{3.26}$$

This joint probability can be used to compute the mean conditional information entropy

$$H(Q_{k+1}|Q_k) = -\sum_{\alpha_k, \alpha_{k+1}} P(\alpha_{k+1}, \alpha_k)\log_2\left(\frac{P(\alpha_{k+1}, \alpha_k)}{P(\alpha_k)}\right). \tag{3.27}$$

Here α_k is a particular realization of the random variable Q_k. For a neutrino born in flavor state $|\nu_\alpha\rangle$ at time t_0, we have $\rho(t_0) = |\nu_\alpha\rangle\langle\nu_\alpha|$, and

$$\begin{aligned} H(Q_{t_1}|Q_{t_0}) &= H[\nu(t_1)|\nu(t_0) = \nu_\alpha] \\ &= -\mathcal{P}_{\alpha\alpha}(t_1 - t_0)\log_2\mathcal{P}_{\alpha\alpha}(t_1 - t_0) \\ &\quad - \sum_{\beta\neq\alpha}\big[\mathcal{P}_{\alpha\beta}(t_1 - t_0)\log_2\mathcal{P}_{\alpha\beta}(t_1 - t_0)\big]. \end{aligned} \tag{3.28}$$

Here $\mathcal{P}_{\alpha\alpha}(t_1 - t_0)$ and $\mathcal{P}_{\alpha\beta}(t_1 - t_0)$ stand for the survival and transition probabilities, respectively.

Given an ensemble of identically prepared neutrinos at time t_0, and considering the preparation step as the first measurement, we can perform a series of measurements, for (say) $N = 3$, such that on the first set of runs, the measurement is performed at time t_1; only at t_1 and t_2 on the second set of runs and at t_2 on the third run ($t_2 > t_1 > t_0$). For measurements carried out at equal time intervals $\Delta t = t_{i+1} - t_i$, $i = 1, 2, \ldots, n$, the survival and oscillation probabilities depend only on the time difference Δt. We define a dimensionless parameter ϕ, which is related to Δt as $\phi = (\Delta_{21}\Delta t)/(2\hbar E)$, where $\Delta_{21} = m_2^2 - m_1^2$ is the mass squared difference and E is the energy of the neutrino.

As an example, the mean conditional information, when the initial state at time t_0 is chosen to be $|\nu_e\rangle$, as a function of ϕ has the following form:

$$\begin{aligned} H[\nu(t_1)|\nu(t_0) = \nu_e](\phi) \\ = -\mathcal{P}_{ee}(\phi)\log_2\mathcal{P}_{ee}(\phi) - \big[\mathcal{P}_{e\mu}(\phi)\log_2\mathcal{P}_{e\mu}(\phi) + \mathcal{P}_{e\tau}(\phi)\log_2\mathcal{P}_{e\tau}(\phi)\big]. \end{aligned} \tag{3.29}$$

Similarly, one can find the expressions for $H(Q_2|Q_1)$ and $H(Q_2|Q_0)$. It turns out that the actual form of $H(Q_2|Q_1)$ involves probabilities which cannot be measured with the present day neutrino experimental facilities. One can overcome this difficulty by exploiting the stationarity principle [23, 27, 38, 230], which, apart from other conditions demands that if the neutrino is prepared in state n at time $t = 0$, then the conditional probabilities $P(n, t + \tau|n, \tau)$ are invariant under time-translation, i.e., $P(n, t + \tau|n, \tau) = P(n, t|n, 0)$. The inequality so obtained could be called entropic Leggett-Garg type inequality, in consonance with its Leggett-Garg counterparts [27]. From now on, to avoid complexity of notation, we will address the entropic Leggett-Garg type inequality as ELGI.

With the notation $H[\nu(t_j)|\nu(t_i) = \nu_e](\phi) = H(\phi)$, the ELGI given by Eq. (2.37), for the neutrino system, under the stationarity assumption discussed above, becomes

$$\mathcal{D}^{[n]}(\phi) = (n-1)H(\phi) - H((n-1)\phi) \geq 0. \tag{3.30}$$

A violation of this inequality, i.e., $\mathcal{D}^{[n]}(\phi) < 0$, would be a signature of the quantum behavior of the system. This information difference is measured in bits (log to base 2). We have studied this equation for two (Fig. 3.5) and three (Fig. 3.6) flavor scenarios of neutrino oscillations in vacuum. The effect of the number of measurements on the information deficit is depicted in Fig. 3.7. We also study the effect of matter density on the deficit parameter in the context of various neutrino experiments as shown in Fig. 3.8.

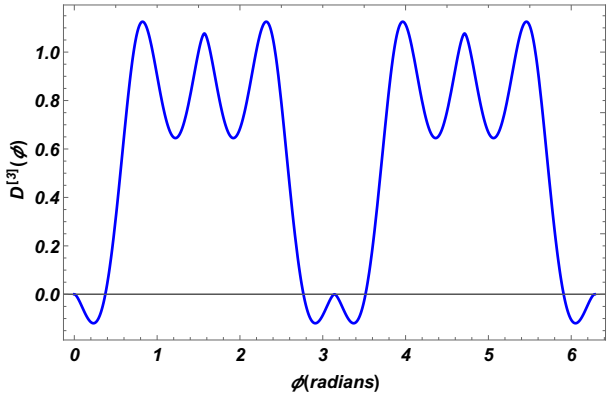

Figure 3.5: Information deficit $\mathcal{D}^{[3]}(\phi)$ plotted against dimensionless parameter $\phi(= (\frac{\Delta_{21}L}{2\hbar cE})$ for *two flavor* approximation in vacuum and three measurements made at t_0, t_1 and t_2 ($t_0 < t_1 < t_2$). The negative values of $D^{[3]}(\phi)$ correspond to the violation of ELGI. The values of the mixing angle θ_{12} and mass squared difference Δ_{21} are chosen to be 33.48^o and $7.5 \times 10^{-5} eV^2$, respectively. The result is independent of the initial state chosen, since the survival and oscillation probabilities have same form irrespective of the initial state. The maximum negative value (measure of the strength of violation) acquired by $\mathcal{D}^{[3]}(\phi)$ is -0.1193.

Wigner and CHSH type of LGI: It turns out that for the case of neutrino system Wigner form of LGI given by inequality (6.65) for the values of $m_1 = -1$, $m_2 = m_3 = +1$ is most suitable. With initial neutrino state $|\nu_\mu\rangle$, let us choose the dichotomic operator $\hat{A} = 2|\nu_e\rangle\langle\nu_e| - \boldsymbol{I}$, where $\boldsymbol{I} = \sum_{\alpha=e,\mu,\tau} |\nu_\alpha\rangle\langle\nu_\alpha|$. The operator $\hat{A}$ amounts to asking whether the neutrino is found in flavor ν_e $(+1)$ or not (-1). With this setting, the standard LGI for three time measurement, turns out to be $K_3 = 1 - 4\mathcal{P}_{\mu e}(t) + 4\mathcal{P}_{ee}(t)\mathcal{P}_{\mu e}(2t) + 4\beta(t)$, Eq. (3.18), where $\beta(t)$ is a non-measurable term [263]. It is worth noting here that for subatomic systems less number of measurements are preferable due to experimental constraints. Therefore, three time LGI is most relevant for such systems. In contrast to the standard LGI, one of the variants of Wigner form of LGI (denoted here by W_Q) turns out to

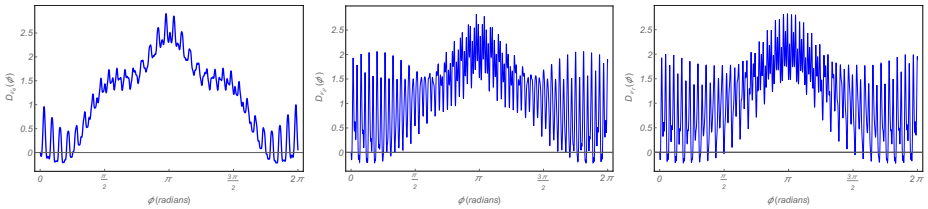

Figure 3.6: Three flavor scenario in vacuum. Information deficit $\mathcal{D}_{\nu_x}^{[3]}(\phi)(x = e, \mu, \tau)$ plotted against dimensionless parameter $\phi(= (\frac{\Delta_{21}L}{2\hbar cE})$. The various neutrino parameters used are as: $\theta_{12} = 33.48^o$, $\theta_{13} = 8.50^o$, $\theta_{23} = 42.3^o$, $\Delta_{21} = 7.5\times10^{-5}\, eV^2$, $\Delta_{32} = \Delta_{31} = 2.457\times10^{-3}\, eV^2$. Left, middle and right figures correspond to the cases with initial state ν_e, ν_μ and ν_τ, respectively. The maximum negative value of the information difference is a measure of the strength of the entropic violation and in this case, turn out to be $Min[\mathcal{D}_e^{[3]}(\phi)] \approx -0.2196$ at $\phi \approx 5.7527\, radians$, $Min[\mathcal{D}_\mu^{[3]}(\phi)] \approx -0.2151$ at $\phi \approx 5.7527\, radians$, $Min[\mathcal{D}_\tau^{[3]}(\phi)] \approx -0.2189$ at $\phi \approx 5.7527\, radians$.

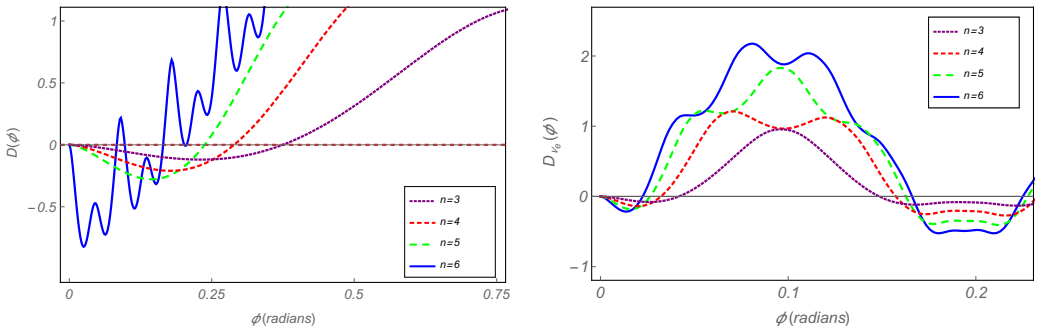

Figure 3.7: Information difference $\mathcal{D}^{[n]}(\phi)$ plotted against dimensionless parameter ϕ for different values of n, the number of observations made on the system. The left and right panels correspond to the two and three flavor cases, in vacuum, respectively. It is clear that, as the number of measurements n increases, the information difference becomes more and more negative. In other words, the maximum negative value of $\mathcal{D}^{[n]}(\phi)$ increases with the increase in the number of measurements. The subscript ν_e shows that the initial state for the three flavor case is chosen to be $|\nu_e\rangle$.

be independent of non-measurable terms and can be shown to be

$$W_Q = \mathcal{P}_{ee}(t)\mathcal{P}_{\mu e}(t) - \mathcal{P}_{\mu e}(2t) \leq 0. \tag{3.31}$$

Here, $\mathcal{P}_{\alpha\beta}(t)$ is the probability of transition from flavor state ν_β to ν_α at time t. This is a remarkable coincidence which has the potential to have positive impact on experimental investigations in the context of LGI violations in neutrino oscillations. The behavior of W_Q defined above is shown in Fig. 3.9.

The suitable Clauser-Horne form of LGI, can be found from the inequality (2.29) for the values of $m_1 = +1$, $m_2 = m_3 = -1$ and is denoted by CH_Q

$$CH_Q = -\mathcal{P}_{\mu e}(t) + \mathcal{P}_{ee}(t)\mathcal{P}_{\mu e}(2t) \leq 0. \tag{3.32}$$

Another useful Clauser-Horne form of LGI, CH'_Q, can be obtained from the inequality

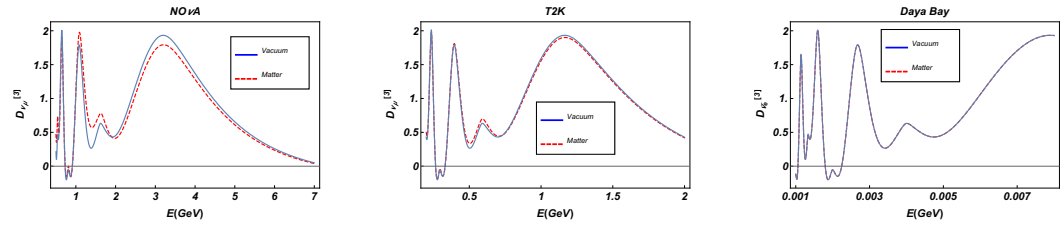

Figure 3.8: Information deficit $\mathcal{D}^{[3]}$ as a function of neutrino energy in three flavor scenario of neutrino oscillation. Left, middle and right plots correspond to NOνA, T2K and Daya-Bay experiments, respectively. Solid and dashed curves show the variation of $\mathcal{D}^{[3]}$ in matter and vacuum, respectively. The baseline for NOνA experiments is 810 km and the energy of the neutrinos varies between 0.5 GeV to 10 GeV. For T2K experiment, the neutrinos pass through a baseline of 295 km with the energy upto 2 GeV. While as in Daya-Bay experiment, neutrino energy is of the order of few MeVs. It is clear that the matter effect is prominent in long baseline and high energy experiments like NOνA than in the small baseline and low energy experiments (T2K and Daya-Bay). The initial flavor in both the accelerator experiments NOνA and T2K is ν_μ, while in the reactor Daya-Bay experiment, the initial state is the electron anti-neutrino $\bar{\nu}_e$.

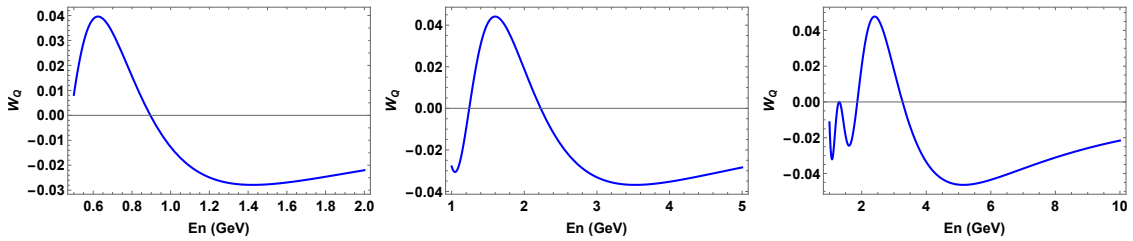

Figure 3.9: Wigner form of LGI (bottom panel) (Eq. (3.31)) in neutrino system for different experimental set ups vz., $T2K$ (left), $NO\nu A$ (middle) and DUNE (right), plotted with respect to the neutrino energy (En) in GeV. The baseline of 295 km, 810 km and 1300 km are used for $T2K$, $NO\nu A$ and DUNE experiments, respectively. The CP violating parameter $\delta = 0$ and the matter density parameter $A \approx 1.01 \times 10^{-13}$ eV.

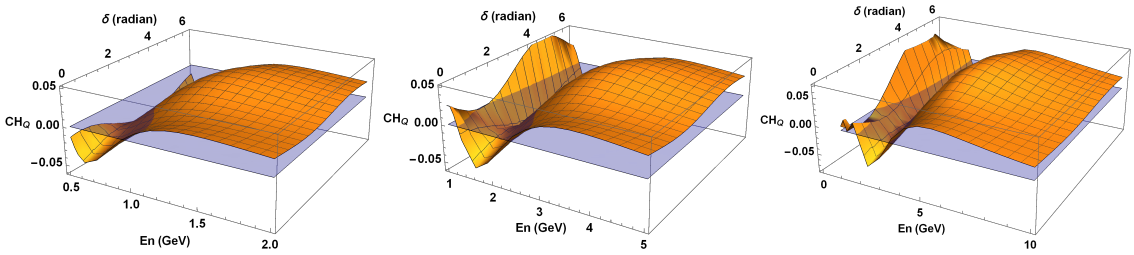

Figure 3.10: Clauser-Horne form of Legget-Garg inequality, Eq.(3.32), in neutrino system for different experimental set ups vz., $T2K$ (left), $NO\nu A$ (middle) and DUNE (right). The quantity CH_Q is plotted with respect to the neutrino energy E_n and the CP violating phase δ.

(2.31) for the values of $m_1 = m_3 = -1, m_2 = +1$

$$CH'_Q = \mathcal{P}_{\mu e}(t) - \mathcal{P}_{\mu e}(2t)[\mathcal{P}_{\mu e}(t) + \mathcal{P}_{\tau\mu}(t)] + \mathcal{P}_{\mu\mu}(2t) + \mathcal{P}_{\tau\mu}(2t) - 1 \leq 0. \tag{3.33}$$

The expressions for various probabilities appearing in the above equations can be seen from [55, 263]. Figures 3.10 and (3.11) depict the behavior of CH_Q and CH'_Q, respectively.

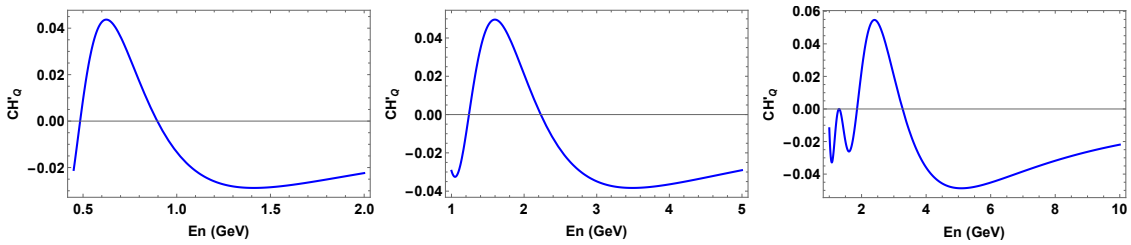

Figure 3.11: Clauser-Horne form of Legget-Garg inequality in neutrino system for energy and baseline corresponding to different experimental set ups vz., $T2K$ (left), $NO\nu A$ (middle) and DUNE (right). The quantity CH'_Q given by Eq. (3.33) is plotted with respect to the neutrino energy E_n. The presence of term $\mathcal{P}_{\tau\mu}$ makes the experimental verification of this quantity difficult in contrast to the scenario depicted by Eq. (3.32).

Here, it is important to note that the quantum violation of the Clauser-Horne form of LGI given by inequality (3.33) is larger than the violation shown by the inequality (3.32) and the Wigner form of LGI (inequality(3.31)) for the experimental set-up of DUNE. It is worth mentioning that $\mathcal{P}_{\alpha\beta}(t)$ depend, apart from time, on parameters like mixing angles, mass square difference, energy of the neutrino and CP violating phase (for $\alpha \neq \beta$). In the ultra-relativistic limit, time can be approximated by the distance it travels, i.e., $t \approx L$. Therefore, the Wigner parameter W_Q becomes a function of L and $2L$. This implies that an experimental verification of this inequality would require two detectors to be placed at L and $2L$, respectively. However, in the present day experimental setups, such a provision is not possible. This difficulty can be bypassed by replacing the $2L$ dependence by L in such a way that $\mathcal{P}_{\mu e}(2L, E) = \mathcal{P}_{\mu e}(L, \tilde{E})$ for energy $\tilde{E}$ within the experimentally allowed range. Such an approach has been used to study Leggett Garg inequality in the context of experimental facilities like NOνA, T2K and DUNE [264]. It should be noted that for vacuum oscillations, energies E and $\tilde{E}$ are related by $\tilde{E} = E/2$. However, this relation is not retained in the presence of matter effects. Given that the matter modified oscillation probability is a smooth function of energy, it is always possible to find at least one $\tilde{E}$ which satisfies the above relation. More explicitly, the solution of $\mathcal{P}_{\mu e}(2L, E) = \mathcal{P}_{\mu e}(L, \tilde{E})$ is obtained for a given value of the CP violating phase within the energy window of the experimental setup. This obviously requires enough neutrino flux to make $\tilde{E}$ fall within the experimental regime. The DUNE experiment which has higher energy range is best suited for this approach.

In contrast to the standard LGI, an attractive feature of the Wigner and Clauser-Horne forms of LGI is that they can be expressed completely in terms of measurable probabilities, as seen in (3.31), (3.32), and (3.33), without invoking the stationarity assumption. However, (3.33) involves transition probabilities from flavor ν_μ to ν_τ, which are beyond the scope of present experimental capabilities. The Wigner and Clauser-Horne forms of LGI may be advantageous over the standard LGI, since the maximum violation occurs at energies around the maximum neutrino flux.

2. Temporal quantum correlations in meson system

Let us assume that at time $t = 0$, the meson was in state $\rho_{\bar{B}^0}$. This state evolves to $\rho_{\bar{B}^0(t_i)}$ at time t_i and is given by Eq. (3.14). We define the dichotomic operator $\Pi = \Pi^+ - \Pi^- = \Pi_{B^0} - (\Pi_{\bar{B}^o} + \Pi_0)$, where $\Pi_x = |x\rangle\langle x|$. Now

$$p(^+t_i) = Tr\{\Pi^+ \rho_{\bar{B}_0}(t_i)\} = [\rho_{\bar{B}_0}(t_i)]_{11} = |p/q|^2 \frac{e^{-\Gamma t_i}}{2}\left[\cosh(\frac{\Delta\Gamma t_i}{2}) - e^{-\lambda t_i}\cos(\Delta m t_i)\right]. \tag{3.34}$$

Thus, $p(^{+}t_i) = \mathcal{P}_{\bar{B}^0 B^0}(t_i)$ is the transition probability from state $\rho_{\bar{B}^0}$ to ρ_{B^0} at time t_i. With the assumption of equal time measurements $t_2 - t_1 = t_1 - 0 = \Delta t$, we have the following expression for C_{12}

$$C_{12} = 1 - 4\mathcal{P}_{\bar{B}^0 B^0}(\Delta t) + 4Re[g(\Delta t)], \tag{3.35}$$

with

$$g(t_1, t_2) = 2\mathcal{P}_{\bar{B}^0 B^0}(\Delta t)\mathcal{P}_{\bar{B}^0 \bar{B}^0}(\Delta t) + |\frac{p}{q}|^2 \frac{e^{-2\Gamma\Delta t}(e^{-2\lambda\Delta t} - 1)}{4}. \tag{3.36}$$

Here $\mathcal{P}_{\bar{B}^0 \bar{B}^0}(\Delta t)$ and $\mathcal{P}_{\bar{B}^0 B^0}(\Delta t)$ are the survival and transition probabilities, respectively, for the meson which started in state $\rho_{\bar{B}^0} = |\bar{B}^0\rangle \langle \bar{B}^0|$ at time $t = 0$. The survival probability of $\bar{B}^o$ has the following form:

$$\mathcal{P}_{\bar{B}^0 \bar{B}^0}(t) = \frac{e^{-\Gamma t}}{2}\left[\cosh(\frac{\Delta\Gamma t}{2}) + e^{-\lambda t}\cos(\Delta m t)\right]. \tag{3.37}$$

The LG function finally becomes

$$K_3 = 1 - 4P_{\bar{B}^0 B^0}(\Delta t) + 8P_{\bar{B}^0 B^0}(\Delta t)P_{\bar{B}^0 \bar{B}^0}(\Delta t) + |p/q|^2 e^{-2\Gamma\Delta t}\big(e^{-2\lambda\Delta t} - 1\big). \tag{3.38}$$

CP violation implies that $|p/q| \neq 1$. The above developed formalism also applies to the K meson case with some notational changes. The CP violating parameter for K mesons ϵ can be expressed in terms of p and q by the following relation $\epsilon = \frac{p-q}{p+q}$.

Stationarity assisted LGI: Given that the state of the meson at time $t = 0$ is $|\bar{B}^o\rangle$, it can be shown that Markovian dynamics described by the Kraus operators in Sec. 3.1 lead to the time translation invariance of the conditional probability, i.e., $P(\bar{B}^o, t + t_0|\bar{B}^o, t_0) = P(\bar{B}^o, t|\bar{B}^o, 0)$. With the assumption of stationarity, the Leggett Garg type inequality, Eq. (2.25), becomes

$$\tilde{K_3} = 1 - 4P_{\bar{B}^o B^o}(\Delta t) + 2P_{\bar{B}^o B^o}(2\Delta t). \tag{3.39}$$

Therefore, a knowledge of the transition probabilities at times Δt and $2\Delta t$ would allow one to compute K_3 according to Eq. (3.39), such that $\tilde{K_3} > 1$ shows the nonclassical nature of the neutral meson oscillations. It should be noted that Eq. (3.39) is expressed completely in terms of directly measurable quantities such as transition probabilities unlike Eq. (3.38), which contains a term $(|p/q|^2 e^{-2\Gamma\Delta t}\big(e^{-2\lambda\Delta t} - 1\big))$, apart from the survival and transition probabilities. However, it can be seen that in the limit of neglecting decoherence effects, Eq. (3.38), can also be expressed directly in terms of survival and transition probabilities.

The experiments on the $B^0(K^0)$ meson systems involve determination of their flavor at the time of production or decay. This is done by analyzing the flavor specific decays. For e.g., a B_d^0 meson can decay into a positron (or a μ^+), a neutrino and a hadron with a branching ratio of ~ 0.1. This semileptonic decay is induced by the quark level transition $\bar{b} \to \bar{c}\, l^+ \nu_l$, with $l = e,\ \mu$. On the other hand, the corresponding decay of a $\bar{B_d^0}$ meson results in an electron (or a μ^-) in the final state. Thus, in general, the charge of the final state lepton is same as the charge of the decaying quark. This is known as the $\Delta B = \Delta Q$ rule for the semileptonic decays of B mesons and is assumed in most of the experimental analysis. Hence, the charge of the final state lepton in the semi-leptonic decays of a neutral meson usually determines the flavor of that meson at the time of decay.

The process of determination of the initial flavor of a neutral meson is called tagging. This is achieved by making use of the rule of associated production. The mesons are produced

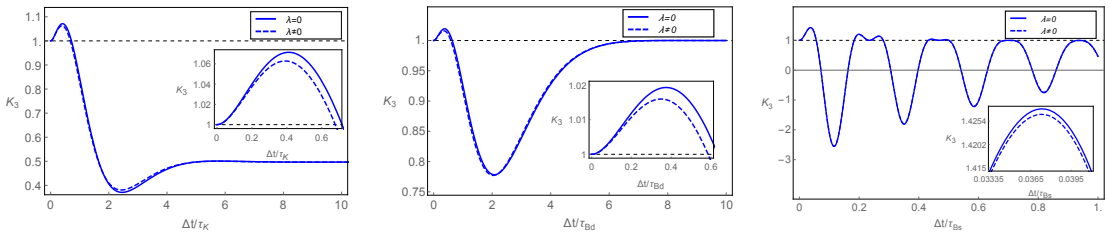

Figure 3.12: The left, middle and right panels of the figure depict the LG function K_3 plotted *w.r.t* the dimensionless quantity $\Delta t/\tau$ for the K, B_d and B_s mesons, respectively. Here Δt is the time between successive measurements and τ is the mean lifetime of respective mesons. Dashed and solid curves correspond to the cases with and without decoherence, respectively. For the K system, the mean lifetime is $\tau_K = 1.7889 \times 10^{-10} s$. Also, $\Gamma = 5.59 \times 10^9$ s^{-1}, $\Delta\Gamma = 1.1174 \times 10^{10}$ s^{-1}, $\lambda = 2.0 \times 10^8$ s^{-1} and $\Delta m = 5.302 \times 10^9$ s^{-1} [265]. Here use has been made of $Re(\epsilon) = 1.596 \times 10^{-3}$ and $|\epsilon| = 2.228 \times 10^{-3}$ [266]. For the B_d system, $\tau_{B_d} = 1.518 \times 10^{-12} s$, $\Gamma = 6.58 \times 10^{11}$ s^{-1}, $\Delta\Gamma = 0$, $\lambda = 0.012 \times 10^{12}$ s^{-1} and $\Delta m = 0.5064 \times 10^{12}$ s^{-1} [267]. The CP violating parameter used here is $|\frac{q}{p}| = 1.010$ [267]. Finally, for the B_s meson, $\tau_{B_s} = 1.509 \times 10^{-12} s$, $\Gamma = 0.6645 \times 10^{12}$ s^{-1}, $\Delta\Gamma = 0.086 \times 10^{12}$ s^{-1}, $\lambda = 0.012 \times 10^{12}$ s^{-1} and $\Delta m = 17.757 \times 10^{12}$ s^{-1} [267]. The value of the CP violating parameter here is $\frac{q}{p} = 1.003$ [267]. As we do not have any experimental bound on the decoherence parameter λ for the B_s system, we assume it to be the same as that of the B_d system.

either by strong or electromagnetic interactions and hence a quark is always produced in association with its anti-quark as flavor is conserved in these interactions. Thus, if a quark q is detected at one end of the detector then at the quark at the other end has to be $\bar{q}$. Now if a charged meson is produced in association with a neutral meson, then the decay of the charged meson determines the flavor of the neutral meson at production. This is so because the charged meson cannot oscillate. The survival and oscillation probability of the neutral meson can then be measured by identifying the charge of the lepton in its semileptonic decay. If two entangled neutral mesons are produced, as in the e^+e^- colliders by the process $e^+e^- \rightarrow \Upsilon(4S) \rightarrow B_d^0 \bar{B}_d^0$, then detecting the flavor specific final state of one meson, say at time t_1, determines the flavor of that meson as well as the other meson at that time t_1. The oscillation probability of the tagged meson is then determined by identifying its final flavor specific state.

The left panel of Fig. 3.12 shows the variation of the LG function K_3, as a function of the dimensionless quantity $\Delta t/\tau_K$. It can be seen from the left panel of the figure that the LG inequality, in K mesons, is violated for about $\Delta t = \tau_K$. The middle and right panels of Fig. 3.12 depict the variation of the LG function for the B_d and B_s mesons, respectively. One can see that the violation in the B_d meson system sustains for about $\Delta t = \tau_{B_d}$ while for the B_s meson system the violation is roughly for $\Delta t \approx 0.5\, \tau_{B_s}$. The maximum violation of LGI occurs around $\Delta t \approx 0.41\tau_K$, $\Delta t \approx 0.37\tau_{B_d}$ and $\Delta t \approx 0.037\tau_{B_s}$ for K, B_d and B_s meson systems, respectively.

The figures clearly bring out the point that from the genesis of its decay [259], the meson systems violate the upper threshold value of $K_3 = 1$, indicative of quantum behavior, and quickly fall below one. The K_3 value for K meson remains above one longest while B_s does it for the shortest time. In addition, the B_s meson exhibits an additional recurrence behavior.

In order to have an understanding of this recurrence behavior, lets re-write Eq. (3.38) as

$$K_3 = 1 + |p/q|^2 \Big[2e^{-(\Gamma+\lambda)\Delta t} \cos(\Delta m \Delta t) - e^{-2(\Gamma+\lambda)\Delta t} \cos(2\Delta m \Delta t) - 2e^{-\Gamma \Delta t} \cosh(\Delta\Gamma \Delta t/2) + e^{-2\Gamma\Delta t} \cosh(\Delta\Gamma\Delta t) \Big]. \tag{3.40}$$

One can then see that the oscillating behavior in the case of B_s meson system could be attributed to the mass term Δm (Eq. (3.40)), which plays the role of frequency, and is more than 35 times the corresponding value for the B_d meson system.

From Eq. (3.39), we find that the LG-type inequality is in terms of the transition probabilities only. Fig. 3.13 shows the deviation of the LG-type function, $\tilde{K_3}$ (3.39), from the LG-function (K_3). It is clear from the figure that the deviation is very small. Thus, a study of the LG inequality in mesons, using $\tilde{K_3}$, Eq. (3.39), in terms of experimentally measurable quantities would be well justified. Eq. (3.39) demands the knowledge of the transition probabilities at Δt and $2\Delta t$, for example, $(0.5\tau_K, \tau_K)$ for the K meson system.

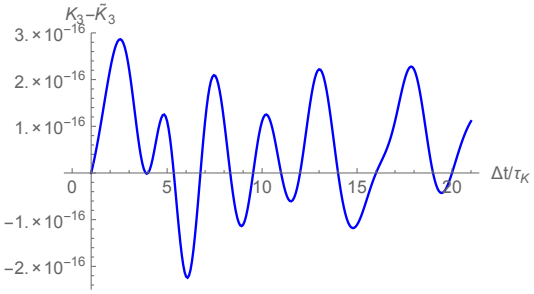

Figure 3.13: Plot of the difference of LG-function K_3 and LG-type function $\tilde{K_3}$ in the case of K meson system. The various parameters used are the same as in Fig. 3.12.

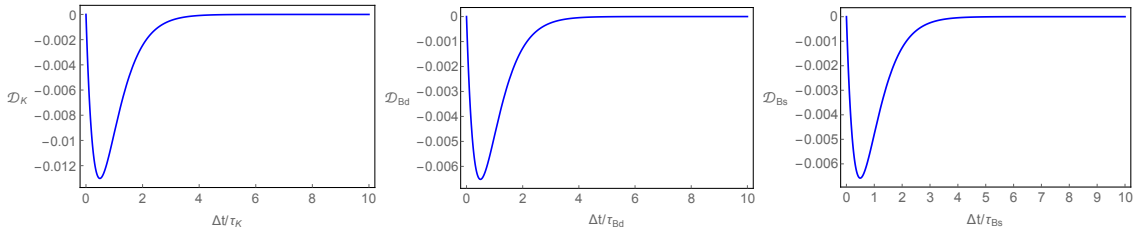

Figure 3.14: The non-measurable term $\mathcal{D}_K = |(1+\epsilon)/(1-\epsilon)|^2 e^{-2\Gamma\Delta t}\left(e^{-2\lambda\Delta t} - 1\right)$ for K-meson system and $\mathcal{D}_{Bd(s)} = |p/q|^2 e^{-2\Gamma\Delta t}\left(e^{-2\lambda\Delta t} - 1\right)$ for $B_{d(s)}$-meson system, plotted against $\Delta t/\tau_{K/B_{d(s)}}$. The various parameters used in the two cases are the same as mentioned in the caption of Fig. 3.12.

Looking at the form of Eq. (3.38), it can be seen that the only non-measurable term in the equation is $|p/q|^2 e^{-2\Gamma\Delta t}\left(e^{-2\lambda\Delta t} - 1\right)$; we call this term $\mathcal{D}_B$ and $\mathcal{D}_K$ for the case of B meson and K meson systems, respectively. In the limit of zero decoherence, $\lambda \to 0$, $\mathcal{D}_{B/K} \to 0$, rendering the LG function, Eq. (3.38), in terms of measurable survival and transition probabilities

$$K_3(\lambda = 0) = 1 - 4P_{\bar{B}^0 B^0}(\Delta t) + 8P_{\bar{B}^0 B^0}(\Delta t) P_{\bar{B}^0 \bar{B}^0}(\Delta t). \tag{3.41}$$

The variation of $\mathcal{D}_B$ and $\mathcal{D}_K$ with $\Delta t/\tau_{K/B_{d(s)}}$ is shown in Fig. 3.14. It is obvious from the figure that these terms are small compared with the maximum value attained by the LG function K_3.